

Synthesis, Structure, and Reactivity of Aliphatic Primary Nitrosamines Stabilized by Coordination to $[\text{IrCl}_5]^{2-}$

Florencia Di Salvo,[†] Darío A. Estrin,[†] Gregory Leitus,[‡] and Fabio Doctorovich^{*†}

Departamento de Química Inorgánica, Analítica y Química Física/INQUIMAE-CONICET, Facultad de Ciencias Exactas y Naturales, Universidad de Buenos Aires, Ciudad Universitaria, Pabellón II, piso 3, C1428EHA Buenos Aires, Argentina, and Department of Chemical Services, The Weizmann Institute of Science, Rehovot 76100, Israel

Received October 2, 2007

In the present work the formation of several primary aliphatic coordinated nitrosamines by reaction of the extremely reactive $\text{K}[\text{IrCl}_5(\text{NO})]$ in acetonitrile solution with the corresponding amine is described. Complete characterization, including X-ray diffraction determinations for some examples, are reported, and experimental evidence of their stability. Density functional theory calculations (DFT) helped to understand the role of the coordination environment of these complexes and to support, with excellent correlation with the experimental data, the proposed reaction pathways and stability studies. Complexes containing the highly unstable primary nitrosamines as ligands are generally scarce, and moreover, to our knowledge, our group has recently reported the first examples of isolated primary nitrosamines coordinated to the metal center only through the NO moiety.

Introduction

Secondary nitrosamines ($\text{R}_1\text{R}_2\text{NN}=\text{O}$) were first described in the chemical literature over 150 years ago, but not until the 1960s did they receive much attention, when positive carcinogenic studies were reported.¹ These are very stable compounds that are obtained when typical nitrosating agents² react with secondary amines.³ For example, they can be found in foods, tobacco products, and *in vivo*. Endogenous generation takes place by the nitrosation of amines in the body, via acid- or bacterial-catalyzed reactions, with nitrite or oxidative products of NO. In foods, they can be formed when amines react with nitrite salts, which are used as a common preservative.⁴ In tobacco products, many specific nitrosamines were found, and several studies indicate their activity as chemical carcinogens.⁵

On the other hand, primary nitrosamines ($\text{R}_1\text{N}(\text{H})\text{N}=\text{O}$) are very unstable and together with their tautomeric isomers, diazoic acids ($\text{R}_1\text{N}=\text{NOH}$), are considered important intermediates in the deamination of DNA bases⁶ and in the formation of diazonium salts.⁷ When nitrous acid (HNO_2) reacts with guanine, adenine, and cytosine, it causes deamination and interstrand cross-linked products. These alterations represent one of the most abundant sources of endogenous DNA damage, and it constitutes a relevant portion of injuries in various disease stages via mutagenesis and cytotoxicity.⁸ Deamination of cytosine and

adenine gives exclusively uracil and hypoxanthine, whereas guanine gives rise to several byproducts.⁹ The direct observation by LC/MS of the diazoate of 2'-deoxycytidine was reported by Makino et al.,¹⁰ but there is no information about the isolation of diazo intermediates obtained by nitrosation reactions of nucleobases.

Aromatic diazonium ions have been known for a long time, showing multiple applications in synthesis, covering a large area of organic chemistry.¹¹ On the contrary, the closely related diazonium ions attached to sp^3 carbons have been very elusive, and except for a few examples observed at low temperature,⁶ only rearranged and nucleophilic attack products are observed when aliphatic amines are nitrosated with different nitrosating agents (Scheme 1). Our group has previously explored the possibility of obtaining stabilized coordinated diazonium ions by reaction of nitrosyl complexes with aromatic and aliphatic primary amines,¹² a route previously pointed out by Meyer et al.,¹³ who isolated coordinated aromatic diazonium salts. In the case of the reaction of $[\text{Fe}(\text{CN})_5\text{NO}]^{2-}$ (nitroprusside) and $[\text{Ru}(\text{bpy})_2(\text{NO})\text{Cl}]^{2+}$ with aliphatic amines, only organic products derived from nucleophilic attack to the diazonium ion or the carbocation could be obtained (bottom part of Scheme 1).¹² However, quantitative analysis of the rearranged/unrearranged products ratio allowed an estimation of the diazo intermediate relative stability. For example, the main organic product derived

* E-mail: doctorovich@qi.fcen.uba.ar.

[†] Universidad de Buenos Aires.

[‡] The Weizmann Institute of Science.

(1) Magee, P. N.; Barnes, J. M. *Br. J. Cancer* **1956**, *10*, 114.

(2) These agents include N_2O_4 , ClNO, BuONO, NO^+ , and acidified NO_2^- salts; see: Lee, J.; Chen, L.; West, A. H.; Richter-Addo, G. B. *Chem. Rev.* **2002**, *102*, 1019.

(3) Mirvish, S. S. *Toxicol. Appl. Pharmacol.* **1975**, *31*, 325.

(4) Ridd, J. H. *Q. Rev. Chem. Soc.* **1961**, *15*, 418.

(5) Hecht, S. S. *Chem. Res. Toxicol.* **1998**, *11*, 1998–560.

(6) Caulfield, J.; Wishnok, J.; Tannenbaum, S. *J. Biol. Chem.* **1998**, *273* (21), 12689.

(7) (a) Mohrig, J. R.; Keegstra, K. *J. Am. Chem. Soc.* **1967**, *89*, 5492.

(b) Berner, D.; McGarrity, J. F. *J. Am. Chem. Soc.* **1979**, *101*, 3135.

(8) Rayat, S.; Wu, Z.; Glaser, R. *Chem. Res. Toxicol.* **2004**, *17*, 1998–1157.

(9) Glaser, R.; Rayat, S.; Lewis, M.; Son, M.; Meyer, S. *J. Am. Chem. Soc.* **1999**, *121*, 6108–6119, and references therein.

(10) Suzuki, T.; Nakamura, T.; Yamada, M.; Ide, H.; Kanaori, K.; Tajima, K.; Morii, T.; Makino, K. *Biochemistry* **1999**, *38*, 7151.

(11) Patai, S. *The Chemistry of Diazonium and Diazo Groups*; Wiley: New York, 1978.

(12) (a) Doctorovich, F.; Trápani, C. *Tetrahedron Lett.* **1999**, *40*, 4635.

(b) Doctorovich, F.; Escola, N.; Trápani, C.; Estrin, D. A.; Turjansky, A. G.;

González Lebrero, M. C. *Organometallics* **2000**, *19*, 3810. (c) Doctorovich,

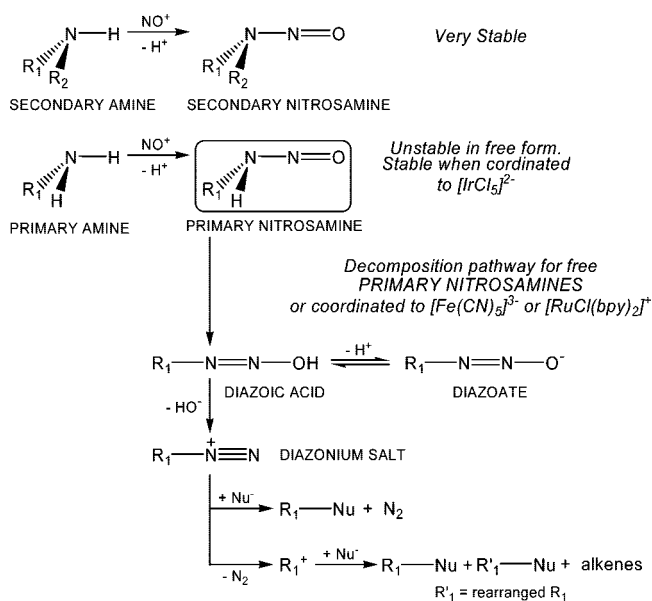
F.; Granara, M.; Di Salvo, F. *Transition Met. Chem.* **2001**, *26*, 505. (d)

Trápani, C.; Escola, N.; Doctorovich, F. *Organometallics* **2002**, *21* (10),

2021–2023. (e) Di Salvo, F.; Crespo, A.; Estrin, D. A.; Doctorovich, F. *Tetrahedron* **2002**, *58*, 4237.

(13) Bowden, W. L.; Little, W. F.; Meyer, T. J. *J. Am. Chem. Soc.* **1977**, *99*, 4340.

Scheme 1. Formation of Aliphatic *N*-Nitrosamines: Stable Secondary Nitrosamines vs Unstable Primary Nitrosamines (for the last case, equilibrium and decomposition pathways are shown)



from the reaction of nitroprusside with aliphatic amines is, in most cases, the corresponding diamine (95% for *n*-butylamine and 30% for benzylamine). For the ruthenium nitrosyl complex, alkenes, rearranged alcohols and chlorides, and small quantities of radical oxidation products were observed apart from the organic products derived from the concerted nucleophilic attack (Scheme 1). This fact suggested that the [Fe(CN)₅]³⁻ moiety is more successful in stabilizing the intermediate diazonium ion through back-donation, as supported by DFT calculations.¹²

Recently, we reported the complete characterization, including X-ray crystallography determinations, of an aromatic and an aliphatic coordinated primary nitrosamine by reaction of the extremely reactive K[IrCl₅(NO)] with *p*-toluidine and 2,2,2-trifluoroethylamine, respectively.¹⁴ Examples of complexes containing primary nitrosamines as ligands are generally scarce,¹⁵ and moreover, to our knowledge these examples were the first ones of isolated primary nitrosamines coordinated to the metal center only through the NO moiety. The facile formation and stabilization of coordinated *N*-nitroso compounds, which do not exist in free form, could be achieved thanks to the high electrophilicity (due to very weak back-bonding) and the inertness of the [IrCl₅]²⁻ moiety. These two qualities, generally not compatible, define the anion [IrCl₅(NO)]⁻ as a rather unique reagent.¹⁶ In the present work we show more examples of coordinated primary nitrosamines derived from the aliphatic amines: benzylamine, *n*-butylamine, cyclopropylamine, and the pseudoaromatic amine 9-octyladenine. Some examples of DNA bases and their derivatives as ligands in transition metal

complexes are known as bioorganometallic compounds,¹⁷ so we consider the last example as an application of this reaction to this growing area of bioorganometallic chemistry.

As an interesting addition to the chemical study of these compounds, we also report their stability and derived products when these compounds are subject to nucleophilic attack. In this way, we show how these diazo derivatives could act in a similar way to the aromatic diazonium salts: as stable precursors for organic synthesis.

As it was mentioned before, density functional theory (DFT) calculations performed by our group have shown a great concordance with the experimental results related to the chemistry of nitroso compounds coordinated to transition metal complexes.^{12,18,19} We complement the experimental study by performing computational calculations at the DFT level *in vacuo* and with a continuum solvation model in order to investigate the structure, stability, properties, and the feasibility of the nucleophilic attack reaction pathways for the described nitrosamines and related diazo compounds.

Experimental Section

General Comments. Unless otherwise noted all manipulations were performed with exclusion of oxygen and moisture using standard Schlenk procedures. ¹H and ¹³C NMR spectra were recorded using a Bruker AM500 equipped with a broadband probe. ¹H and ¹³C shifts are reported relative to CD₃CN ($\delta = 1.95$ and 118 ppm, respectively) or to DMSO-*d*₆ ($\delta = 2.50$ and 39.5 ppm, respectively), and correlations were confirmed through 2D and DEPT 135° experiments. ESI-MS (electrospray ionization mass spectrometry) measurements were performed using a high-resolution hybrid quadrupole (Q) and orthogonal time-of-flight (ToF) mass spectrometer (QToF from Micromass, UK) operating in the negative ion electrospray ionization mode set from 2100 to 3500 V; for details see ref 20. IR spectra were recorded using a Nicolet Avatar 320 FTIR spectrometer with a Spectra Tech cell for KBr pellets. UV-visible spectra were recorded using a Hewlett-Packard 8453 diode array spectrometer in 10 mm optical path quartz cuvettes. CHN elemental analysis was made in a Carlo Erba EA 1108 apparatus. GC-mass spectra were recorded on a Shimadzu GC-17A gas chromatograph with a HP Ultra 2 capillary column attached to a GCMS-QP5000 mass spectrometer operating in the positive ion electronic impact ionization mode at 70 eV. Data collection and processing of the X-ray diffraction studies were performed in a Nonius KappaCCD diffractometer, Mo K α ($\lambda = 0.71073$ Å), graphite monochromator, $T = 120(2)$ K. The data were processed with Denzo-Scalepack. Solution and refinement: Structure solved by Patterson method with SHELXS. Full matrix least-squares refinement is based on F^2 with SHELXL-97.

Reagents. Acetonitrile was purchased from J. T. Baker and distilled from CaH₂; toluene was purchased from Cicarelli and distilled from Na-benzophenone. 2,2,2-Trifluoroethylamine, benzylamine, cyclopropylamine, adenine, tetraphenylarsonium chloride, tetraphenylphosphonium bromide, octylbromide, K₃[IrCl₆], Na¹⁵NO₂, deuterated solvents, and acids were purchased from Sigma-Aldrich Argentine and used as received. *n*-Butylamine was purchased from Rieder-de Haën and used as received. K[IrCl₅(NO)]

(14) Doctorovich, F.; Di Salvo, F.; Escola, N.; Trápani, C.; Shimon, L. *Organometallics* **2005**, *24*, 4707.

(15) (a) Schramm, K.; Dahl Schramm; Ibers, J. A. *J. Am. Chem. Soc.* **1978**, *100*, 2932. (b) Keefer, L. K.; Wang, S.; Anjo, T.; Fanning, J. C.; Day, C. S. *J. Am. Chem. Soc.* **1988**, *110*, 2800. (c) Vaughan, G. A.; Chadwick, D. S.; Hillhouse, G. L. *J. Am. Chem. Soc.* **1989**, *111*, 5491–5493. (d) Lalor, F. J.; Desmond, T. J.; Ferguson, G.; Siew, P. Y. *J. Chem. Soc., Dalton Trans.* **1982**, *10*, 1981.

(16) (a) Di Salvo, F.; Escola, N.; Estrin, D. A.; Sherlis, D. A.; Shimon, L.; Doctorovich, F. *Chem.-Eur. J.* **2007**, *13*, 8428. (b) Doctorovich, F.; Di Salvo, F. *Acc. Chem. Res.* **2007**, *40*, 985.

(17) Fish, R. H.; Jaouen, G. *Organometallics* **2003**, *22*, 2166.

(18) Perissinotti, L. L.; Estrin, D. A.; Leitun, G.; Doctorovich, F. *J. Am. Chem. Soc.* **2006**, *128*, 2512.

(19) Escola, N.; Llebaria, A.; Doctorovich, F.; Leitun, G. *Organometallics* **2006**, *25*, 3799.

(20) Escola, N.; Di Salvo, F.; Haddad, R.; Perissinotti, L.; Nogueira Eberlin, M.; Doctorovich, F. *Inorg. Chem.* **2007**, *46*, 4827.

was purchased from Strem, and $\text{K}[\text{IrCl}_5(^{15}\text{N}\text{O})]$ was prepared from $\text{K}_3[\text{IrCl}_6]$ and $\text{Na}^{15}\text{NO}_2$ by known procedures.²¹

General Synthesis of $[\text{IrCl}_5(\text{N-nitrosamines})]^{2-}$. For the preparation of the corresponding coordinated *N*-nitrosamine 3.6 μL (0.046 mmol) of 2,2,2-trifluoroethylamine for the synthesis of $[\text{IrCl}_5(\text{N-nitroso-2,2,2-trifluoroethylamine})]^{2-}$ (**1**), 5.0 μL (0.046 mmol) of benzylamine for $[\text{IrCl}_5(\text{N-nitrosobenzylamine})]^{2-}$ (**2**), 4.6 μL (0.046 mmol) of *n*-butylamine for $[\text{IrCl}_5(\text{N-nitroso-}n\text{-butylamine})]^{2-}$ (**3**), 3.2 μL (0.046 mmol) of cyclopropylamine for $[\text{IrCl}_5(\text{N-nitrosocyclopropylamine})]^{2-}$ (**4**), and 11.4 mg (0.046 mmol) of 9-octyladenine (dissolved in 0.25 mL of acetonitrile) for $[\text{IrCl}_5(\text{N-nitroso-9-octyladenine})]^{2-}$ (**5**) were added under Ar atmosphere at RT to 10 mg (0.023 mmol) of $\text{K}[\text{IrCl}_5(\text{NO})]$ in 0.25 mL of acetonitrile. 9-Octyladenine was prepared from adenine and the corresponding alkyl bromide by known procedures.²² In all cases the resultant product was $\text{K}(\text{NH}_3\text{R})[\text{IrCl}_5(\text{ONNHR})]$, with $\text{R} = -\text{CH}_2\text{CF}_3$ for **1**, $-\text{CH}_2\text{C}_6\text{H}_5$ for **2**, $-\text{C}_4\text{H}_9$ for **3**, $-\text{C}_3\text{H}_5$ for **4**, and $-\text{C}_{13}\text{H}_{19}\text{N}_4$ for **5**; in some cases up to 5% of the ammonium salt was replaced by H^+ , giving a coordinated nitrosamine: ammonium salt ratio of about 1:0.9.

To increase the yield of **3** and **4**, different reaction temperatures were explored. The use of an ethanol–liquid nitrogen slush bath (ca. -35°C) was found to be the best option. In all cases, the product that precipitated immediately was separated from the solution by centrifugation (the counterions are the ammonium salt of the corresponding amine and a potassium ion); the yield obtained for the corresponding product was from 80 to 90% and the precipitate colors were light orange for **1**, **3**, and **4**, yellow for **2**, and dark red for **5**. All nitrosamine products are soluble in only water and DMSO; the last one was chosen for NMR and ESI-MS experiments. The tetraphenylphosphonium salts, $(\text{PPh}_4)_2\text{-}[\text{IrCl}_5(\text{ONNHR})]$, were obtained by adding a saturated aqueous solution of the crude product to an acetonitrile saturated solution of tetraphenylphosphonium bromide. After slow evaporation of the supernatant, the so produced orange crystals were separated by centrifugation and carefully dried. The crystals obtained for the 2,2,2-trifluoroethylamine and benzylamine products were suitable for X-ray analysis.

$[\text{IrCl}_5(\text{N-nitroso-2,2,2-trifluoroethylamine})]^{2-}$ (1**).** Data for the tetraphenylphosphonium salt. ^1H NMR (DMSO): δ 4.42 and 4.43 (q, 2H, $^3J_{\text{HF}} = 9.37$ Hz, $\text{ONNHCH}_2\text{CF}_3$), 13.1 ppm (br s, 0.8H, $\text{ONNHCH}_2\text{CF}_3$), 7.75–8 ppm (m, 42H, 2PPh₄). ^{13}C NMR (DMSO): δ 44.3 (q, $^2J_{\text{CF}} = 35$ Hz, $\text{ONNHCH}_2\text{CF}_3$), 121.3 (q, $^1J_{\text{CF}} = 280$ Hz, $\text{ONNHCH}_2\text{CF}_3$), 130.3, 130.4, 134.4, 134.5, 135.2, 135.3 ppm (s, 2PPh₄). Anal. C = 49.5% (calc 49.5), H = 3.5% (calc 3.9), N = 2.3% (calc 2.3); for the calculated values 2 molecules of water were taken into account, data confirmed by X-ray crystallography and ^1H NMR. See ref 14 for the X-ray crystal structure analysis of this compound.

Data for the potassium and ammonium salt. ^1H NMR (DMSO): δ 3.84 (q, 2H, $^3J_{\text{HF}} = 9.41$ Hz, $^+\text{NH}_3\text{CH}_2\text{CF}_3$), 4.50 (q, 2H, $^3J_{\text{HF}} = 9.37$ Hz, $\text{ONNHCH}_2\text{CF}_3$), 9.31 (br s, 2.5H, $^+\text{NH}_3\text{CH}_2\text{CF}_3$), 13.0 ppm (br s, 0.8H, $\text{ONNHCH}_2\text{CF}_3$). ^{13}C NMR (DMSO): δ 39.86 (q, $^2J_{\text{CF}} = 34.99$ Hz, $^+\text{NH}_3\text{CH}_2\text{CF}_3$), 44.4 (q, $^2J_{\text{CF}} = 34.6$ Hz, $\text{ONNHCH}_2\text{CF}_3$), 122.44 (q, $^1J_{\text{CF}} = 279.74$ Hz, $^+\text{NH}_3\text{CH}_2\text{CF}_3$), 123.53 ppm (q, $^1J_{\text{CF}} = 277.71$ Hz, $\text{ONNHCH}_2\text{CF}_3$). FTIR frequencies: $\nu(\text{HNNO})$ 1547 cm^{-1} , $\nu(\text{HN}^{15}\text{NO})$ 1534 cm^{-1} . UV–visible absorption in water, λ_{max} (ϵ_{max} in $\text{M}^{-1}\text{cm}^{-1}$): 195(2.3×10^4), 321(1.6×10^3), 384(10^3), 436(6.5×10^3). ESI-MS: for $\text{M} = [\text{IrCl}_5(\text{ONN}(\text{H})\text{CH}_2\text{CF}_3)]^{2-}$, $[\text{M} + \text{K}]^- = 536.789$ m/z (calc 536.7877), $[\text{M} - \text{Cl}]^- = 462.853$ m/z (calc 462.9856).²⁰

$[\text{IrCl}_5(\text{N-nitrosobenzylamine})]^{2-}$ (2**).** Data for the tetraphenylphosphonium salt (Ph = phenyl group, C_6H_5). ^1H NMR (DMSO): δ 4.67 and 4.76 (s, 2H, ONNHCH_2Ph), 13.00 (br s, 1H,

$\text{ONNHCH}_2\text{CF}_3$), 7.24–7.34 (m, 5H, ONNHCH_2Ph), 7.72–8 ppm (m, 42H, 2PPh₄). ^{13}C NMR (DMSO): δ 48.5 (s, ONNHCH_2Ph), 127.4–128.5 and 134.6 (ONNHCH_2Ph), 130.4, 130.5, 134.5, 134.6, 135.2, 135.3 ppm (s, 2PPh₄). X-ray crystal structure data: $\text{C}_{55}\text{H}_{48}\text{N}_2\text{O}_4\text{P}_2\text{Cl}_5\text{Ir}$, $(\text{PPh}_4)_2[\text{IrCl}_5(\text{ONNHCH}_2\text{H}_7)] \cdot 3\text{H}_2\text{O}$ (water protons are not included in the X-ray refinement), M_r 1232.34, orange prisms, triclinic, dimensions $0.20 \times 0.10 \times 0.10$ mm^3 , group = $P(-1)$ (#2), $a = 14.034(3)$ Å, $b = 14.109(3)$ Å, $c = 16.251(3)$ Å, $\alpha = 87.69(3)^\circ$, $\beta = 65.47(3)^\circ$, $\gamma = 66.00(3)^\circ$, $V = 2643.0(9)$ Å³, $Z = 2$, $D_x = 1.548$ Mg m^{-3} , $\lambda = 0.71073$ Å, cell parameters from 11 071 reflections, $\theta = 2.886$ mm^{-1} , $T = 120(2)$ K. X-ray crystal collection and refinement: $T_{\text{min}} = 0.5960$, $T_{\text{max}} = 0.7612$, 7588 measured and independent reflections, 6738 reflections with $>2\sigma(I)$, $\theta_{\text{max}} = 23.26^\circ$, $h = -13 \rightarrow 15$, $k = -15 \rightarrow 15$, $l = 0 \rightarrow 18$, refinement based on F^2 , $R = 0.0533$ (for data with $F^2 > 2\sigma(F^2)$), $wR(F^2) = 0.1153$, $S = 1.242$, $R_1 = 0.0619$ on 7588 reflections, 612 parameters, largest electron density peak = 2.638 $\text{e} \cdot \text{Å}^{-3}$, H atoms treated by a mixture of independent and constrained refinement.

Data for the potassium and ammonium salt. ^1H NMR (DMSO): δ 4.04 (s, 2H, $^+\text{NH}_3\text{CH}_2\text{Ph}$), 4.74 and 4.76 (s, 2H, ONNHCH_2Ph), 8.08 (br s, 2.5 H, $^+\text{NH}_3\text{CH}_2\text{Ph}$), 13.1 (br s, 0.6H, $\text{ONNHCH}_2\text{CF}_3$), 7.3–7.4 (m, 5H, $^+\text{NH}_3\text{CH}_2\text{Ph}$), 7.4–7.5 ppm (m, 5H, ONNHCH_2Ph). ^{13}C NMR (DMSO): δ 43.2 (s, $^+\text{NH}_3\text{CH}_2\text{Ph}$), 48.8 (s, ONNHCH_2Ph), 127.4–128.5 and 134.6 ppm (ONNHCH_2Ph and $^+\text{NH}_3\text{CH}_2\text{Ph}$). FTIR frequencies: $\nu(\text{HNNO})$ 1530 cm^{-1} , $\nu(\text{HN}^{15}\text{NO})$ 1508 cm^{-1} . UV–visible absorption in water, λ_{max} (ϵ_{max} in $\text{M}^{-1}\text{cm}^{-1}$): 198(4.2×10^4), 310(1.8×10^3), 377(6×10^3), 429(3×10^3). Anal. C = 24.9% (calc 25.0), H = 2.7% (calc 2.7), N = 6.0% (calc 6.3), calculated values are according to a 1:0.9 coordinated nitrosamine:ammonium salt counterion ratio found by ^1H NMR. ESI-MS: for $\text{M} = [\text{IrCl}_5(\text{ONN}(\text{H})\text{CH}_2\text{C}_6\text{H}_5)]^{2-}$, $[\text{M} + \text{K}]^- = 544.834$ m/z (calc 544.8313), $[\text{M} - \text{Cl}]^- = 470.900$ m/z (calc 470.8990).²⁰

$[\text{IrCl}_5(\text{N-nitroso-}n\text{-butylamine})]^{2-}$ (3**).** The products obtained at RT are mainly $\text{N}_2(\text{g})$, *n*-butylalcohol(sc), $[\text{IrCl}_5(\text{NH}_2\text{-C}_4\text{H}_9)]\text{KNH}_3\text{C}_4\text{H}_9(\text{s})$, and coordinated *N*-nitroso-*n*-butylamine with a yield of 30%. When the reaction is performed at -35°C , the nitrosamine yield increases to 78%.

Data for the potassium and ammonium salt. ^1H NMR (DMSO): δ 0.91 (m, 7H, $^+\text{NH}_3\text{CH}_2(\text{CH}_2)_2\text{CH}_3$ and $\text{ONNHCH}_2(\text{CH}_2)_2\text{CH}_3$), 1.35 (m, 4H, $^+\text{NH}_3\text{CH}_2(\text{CH}_2)_2\text{CH}_3$), 1.52 (m, 4H, $\text{ONNHCH}_2(\text{CH}_2)_2\text{CH}_3$), 2.77 (br t, 2H, $^+\text{NH}_3\text{CH}_2(\text{CH}_2)_2\text{CH}_3$), 3.58 (t, 2H, $^3J_{\text{HH}} = 6.69$ Hz, $\text{ONNHCH}_2(\text{CH}_2)_2\text{CH}_3$), 7.5 (br s, 2.2 H, $^+\text{NH}_3\text{CH}_2(\text{CH}_2)_2\text{CH}_3$), 12.8 ppm (br s, 0.7H, $\text{ONNHCH}_2(\text{CH}_2)_2\text{CH}_3$). ^{13}C NMR (DMSO): δ 13.2 (s, $^+\text{NH}_3\text{CH}_2(\text{CH}_2)_2\text{CH}_3$ and $\text{ONNHCH}_2(\text{CH}_2)_2\text{CH}_3$), 18.9 (s, $^+\text{NH}_3\text{CH}_2(\text{CH}_2)_2\text{CH}_3$), 28.7 and 29.2 (s, $\text{ONNHCH}_2(\text{CH}_2)_2\text{CH}_3$), 38.6 (s, $^+\text{NH}_3\text{CH}_2(\text{CH}_2)_2\text{CH}_3$), 44.9 ppm (s, $\text{ONNHCH}_2(\text{CH}_2)_2\text{CH}_3$). FTIR frequencies: $\nu(\text{HNNO})$ 1535 cm^{-1} , $\nu(\text{HN}^{15}\text{NO})$ 1487 cm^{-1} . UV–visible absorption in DMSO, λ_{max} (ϵ_{max} in $\text{M}^{-1}\text{cm}^{-1}$): 260(2×10^3), 322(2.3×10^2), 363(2.7×10^2), 422(93). Anal. C = 15.7% (calc 15.8), H = 3.4% (calc 3.7), N = 6.9% (calc 7.0), calculated values are according to a 1:0.9 coordinated nitrosamine:ammonium salt counterion ratio found by ^1H NMR. ESI-MS: for $\text{M} = [\text{IrCl}_5(\text{ONN}(\text{H})\text{C}_4\text{H}_9)]^{2-}$, $[\text{M} + \text{K}]^- = 510.834$ m/z (calc 510.8473), $[\text{M} + \text{NH}_3\text{C}_4\text{H}_9]^- = 545.972$ m/z (calc 545.9805).²⁰

$[\text{IrCl}_5(\text{N-nitrosocyclopropylamine})]^{2-}$ (4**).** The products obtained at RT are $\text{N}_2(\text{g})$, *n*-cyclopropylalcohol(sc), several ring-opening alkanes and alkenes derivatives found in solution, and $\text{KNH}_3(\text{c-CHCH}_2\text{CH}_2)[\text{IrCl}_5(\text{CH}_3\text{CN})] \cdot x\text{CH}_3\text{CN}(\text{s})$ in a 50% yield. Characterization data of the solid product: ^1H NMR (DMSO): δ 3.00 ppm (s, coordinated CH_3CN). ^{13}C NMR (DMSO): δ 2.3 and 113.5 ppm (s, coordinated CH_3CN) (see later for the counterion data). Anal. C = 11.9% (calc 11.8), H = 2.3% (calc 2.2), N = 5.8% (calc 5.5); ESI-MS: for $\text{M} = [\text{IrCl}_5(\text{CH}_3\text{CN})]^{2-}$, $[\text{M} - \text{Cl} - \text{AcN}]^- = 332.8319$ m/z (calc 332.8383), $[\text{M} - \text{Cl} + \text{K}]^{--} = 4128429$ m/z

(21) Bottomley, F.; Clarkson, S. G.; Tong, S. B. *J. Chem. Soc., Dalton Trans.* **1974**, 21, 2344.

(22) Bunton, C. A.; Wolfe, B. B. *J. Am. Chem. Soc.* **1974**, 96, 7747.

(calc 412.8286), $[M + K]^- = 488.8628$ m/z (calc 488.8240). When the reaction is performed at -35 °C, the yield of the nitrosamine is 92%.

Data for the potassium and ammonium salt product. ^1H NMR (DMSO): δ 0.60 and 0.72 (m, 4H, $^+\text{NH}_3\text{CH}(\text{CH}_2\text{CH}_2)$), 0.66 and 0.91 (m, 4H, ONNH $\text{CH}(\text{CH}_2\text{CH}_2)$), 2.52 (m, 1H, $^+\text{NH}_3\text{-CH}(\text{CH}_2\text{CH}_2)$), 3.16 (m, 1H, ONNHCH CH_2CH_2), 8.5 (br s, 3H, $^{\pm}\text{NH}_3\text{CHCH}_2\text{CH}_2$), 12.5 ppm (br s, 0.8H, ONNHCH CH_2CH_2). ^{13}C NMR (DMSO): δ 3.8 ($^+\text{NH}_3\text{CH}(\text{CH}_2\text{CH}_2)$), 6.5 (ONNHCH (CH_2CH_2)), 22.9 ($^+\text{NH}_3\text{CH}(\text{CH}_2\text{CH}_2)$), 29.2 ppm (ONNHCH CH_2CH_2). FTIR frequencies: $\nu(\text{HNNO})$ 1410 cm^{-1} , $\nu(\text{HN}^{15}\text{NO})$ 1394 cm^{-1} . UV-visible absorption in DMSO, λ_{max} (ϵ_{max} in $\text{M}^{-1}\text{cm}^{-1}$): 260(2×10^3), 326(6.9×10^2), 353(7×10^2), 379(5.4×10^2), 420(2.6×10^2). Anal. C = 13.2% (calc 13.0), H = 2.7% (calc 2.6), N = 7.3% (calc 7.6).

$[\text{IrCl}_5(\text{N-nitroso-9-octyladenine})]^{2-}$ (**5**). ^1H NMR (DMSO) (data for a complex with a 2:1 coordinated nitrosamine:ammonium salt counterion ratio): δ 0.84 (t, 5 H, CH_3 from C_8H_{17}), 1.4 and 2.0 (m, 21 H, CH_2 from C_8H_{17}), 4.12 (t, 1 H, $^3J_{\text{HH}} = 7.08$ Hz, CH_2 bound to the indol ring in the ammonium salt counterion), 4.28 (t, 2 H, $^3J_{\text{HH}} = 7.08$ Hz, CH_2 bound to the indol ring in the nitrosamine), 7.75 (br s, 2 H, ammonium salt NH_3^+ signal), 8.24 and 8.26 (s, 2 H, indol ring signals of the ammonium salt counterion), 8.64 and 8.74 (s, 2 H, indol ring signals in the nitrosamine), 14.48 ppm (s, 0.7 H, ONNH $\text{C}_{13}\text{H}_{19}\text{N}_4$). ^{13}C NMR (DMSO): δ 13.66 (CH_3 from C_8H_{17}), 21.78, 21.62, 25.62, 28.10, 28.22, 28.94, 30.88 (CH_2 from C_8H_{17}), 43.11 (CH_2 bound to the indol ring of the ammonium salt counterion), 43.4 (CH_2 bound to the indol ring of the nitrosamine), 117.84, 140.01, 145.26, 148.09, 150.68 (C1, C4, C5, C2, C3 indol ring signals in the ammonium salt), 123.38, 143.39, 145.256, 147.29, 148.39 ppm (C1, C4, C5, C2, C3 indol ring signals of the nitrosamine). FTIR frequencies: $\nu(\text{HNNO})$ 1449 and 1438 cm^{-1} , $\nu(\text{HN}^{15}\text{NO})$ 1436 and 1430 cm^{-1} . UV-visible absorption in water, λ_{max} (ϵ_{max} in $\text{M}^{-1}\text{cm}^{-1}$): 263(4.5×10^3), 271(4×10^3), 325(2×10^3), 384(10^3), 427(7×10^2). ESI-MS: for $\text{M} = [\text{IrCl}_5(\text{ONN}(\text{H})\text{C}_{13}\text{H}_{19}\text{N}_4)]^{2-}$, $[\text{M} + \text{HCl}]^- = 610.040$ m/z (calc 609.9975), $[\text{M} - \text{Cl} + \text{H}_2\text{O}]^- = 629.034$ m/z (calc 629.0158).²⁰

Nitrosamine Decomposition Reactions. The decomposition of the nitrosamines after the addition of strong acids was analyzed. The experiments were performed for all the nitrosamines. The acids used in these reactions were acetic, hydrochloric, deuterated hydrochloric, trifluoroacetic, perchloric, and trifluoroacetic acid solutions with sodium iodide. The lifetime of the nitrosamine and appearance of final products was first checked by ^1H NMR and then by GC-MS. For the NMR experiments, the acid was added to a DMSO- d_6 or D_2O solution of the nitrosamine in a 2:1 ratio. GC-MS experiments were made on organic solutions of the decomposition products. These solutions were obtained after extracting with CH_2Cl_2 the organic compounds derived from the addition of acid to a saturated water solution of the corresponding nitrosamine.

Computational Methodology. All gas phase DFT calculations performed in this work were carried out using the GAUSSIAN 98 software package.²³ Unless otherwise indicated, geometries were fully optimized at the B3LYP^{24,25} and/or BPW91²⁶ level with a

double- ζ plus polarization (DZPV) basis set²⁷ for N, O, F, H, and Cl atoms and the LANL2DZ basis set and effective core potential for the metals (Ir, Fe).^{28,29} A normal modes analysis was performed in order to obtain vibrational frequencies, force constants, and zero-point energy corrections for the total energy. Atomic charges have been calculated using the Mulliken and NPA³⁰ schemes. Solvent effects were modeled using a variety of the self-consistent reaction field method (SCRF): the polarized continuum model (PCM) schemes. This model considers that the solute is placed in a cavity of a quite realistic molecular shape. The PCM implementation given in ref 31, in which the self-consistency between the solute wave function and solvent polarization is achieved during the self-consistent-field cycle, has been employed. Solvent calculations were performed on the *in vacuo*-optimized structures using the GAUSSIAN 98 software package.²¹

Results and Discussion

Formation of Nitrosamines. When an amine was added to an acetonitrile solution of $\text{K}[\text{IrCl}_5(\text{NO})]$, immediate formation of the corresponding coordinated nitrosamine precipitate was observed (**1** in the case of 2,2,2-trifluoroethylamine, **2** for benzylamine, **3** for *n*-butylamine, **4** for cyclopropylamine, and **5** for 9-octyladenine); except for **5**, which was a dark red product, the obtained solids were all yellow to light orange colored. For most of the experiments the observed counterions were K^+ and the corresponding ammonium salt. These facts were evidenced by ^1H and ^{13}C NMR and by stoichiometric analysis of the reaction mixture (see Figure 1A). Although in all cases the main product was the solid nitrosamine complex, the stability was different for each compound. Depending on the amine, temperature conditions had to be optimized; 2,2,2-trifluoroethylamine, benzylamine, and 9-octyladenine products were easily obtained at RT or even higher temperatures, but isolation of the nitrosamines derived from *n*-butylamine and cyclopropylamine was only possible at temperatures around -30 °C. For these two cases, the nitrosamines obtained at the very first moment rapidly decomposed at RT, giving more stable products. The evolution of $\text{N}_2(\text{g})$, changes in the solution color, and final appearance of precipitates were clear evidence of this fact. In the case of *n*-butylamine, the observed products were *n*-butyl alcohol and coordinated amine, which precipitated from the media. For cyclopropylamine, several products derived from ring-opening, nucleophilic attack, and elimination reactions were observed in solution and a precipitate was identified as $[\text{IrCl}_5(\text{CH}_3\text{CN})]\text{K}(\text{NH}_3\text{CH}(\text{CH}_2)_2) \cdot x\text{CH}_3\text{CN}$. When the reaction was performed at -35 °C, the results for these two amines were the same as for the other three examples: clean reactions with the generation of a unique product in high yield and easily isolated (see Table 1).

After recrystallization and change of both counterions by tetraphenylphosphonium (PPh_4^+) (Figure 1B), crystals suitable for X-ray diffraction were obtained for the trifluoroethyl (**1**) and benzyl (**2**) derivatives (see Figures 2 and 3 and Experimental Section).

An outstanding characteristic of these compounds is that the nitrosamines are placed in a *syn* arrangement. Fishbein et al. have studied the decay of different free alkanediazoates,

(23) Frisch, M. J.; Trucks, G. W.; Schlegel, H. B.; Scuseria, G. E.; Robb, M. A.; Cheeseman, J. R.; Zakrzewski, V. G.; Montgomery, J. A., Jr.; Stratmann, R.; Burant, J.; Dapprich, S.; Millam, J. M.; Daniels, A. D.; Kudin, K. N.; Strain, M. C.; Farkas, O.; Tomasi, J.; Barone, V.; Cossi, M.; Cammi, R.; Mennucci, B.; Pomelli, C.; Adamo, C.; Clifford, S.; Ochterski, J.; Petersson, G. A.; Ayala, P. Y.; Cui, Q.; Morokuma, K.; Malick, D. K.; Rabuck, A. D.; Raghavachari, K.; Foresman, J. B.; Cioslowski, J.; Ortiz, J. V.; Baboul, A. G.; Stefanov, B. B.; Liu, G.; Liashenko, A.; Piskorz, P.; Komaromi, I.; Gomperts, R.; Martin, R. L.; Fox, D. J.; Keith, T.; Al-Laham, M. A.; Peng, C. Y.; Nanayakkara, A.; Gonzalez, C.; Challacombe, M.; Gill, P. M. W.; Johnson, B.; Chen, W.; Wong, M. W.; Andres, J. L.; Gonzalez, C.; Head-Gordon, M.; Replogle, E. S.; Pople, J. A. *Gaussian 98, Rev. A7*; Gaussian, Inc.: Pittsburgh, PA, 1998.

(24) Becke, A. D. *J. Chem. Phys.* **1988**, *98*, 5648.

(25) Lee, C.; Yang, W.; Parr, R. *Phys. Rev. B* **1998**, *37*, 785.

(26) Becke, A. D. *Phys. Rev. A* **1998**, *38*, 3098.

(27) Godbout, N.; Salahub, D. R.; Andzelm, J.; Wimmer, E. *Can. J. Chem.* **1992**, *70*, 560.

(28) Hay, P. J.; Wadt, W. R. *J. Chem. Phys.* **1985**, *82*, 270.

(29) Wadt, W. R. *J. Chem. Phys.* **1985**, *82*, 299.

(30) Reed, A. E.; Curtis, L. A.; Weinhold, F. *Chem. Rev.* **1988**, *88*, 899.

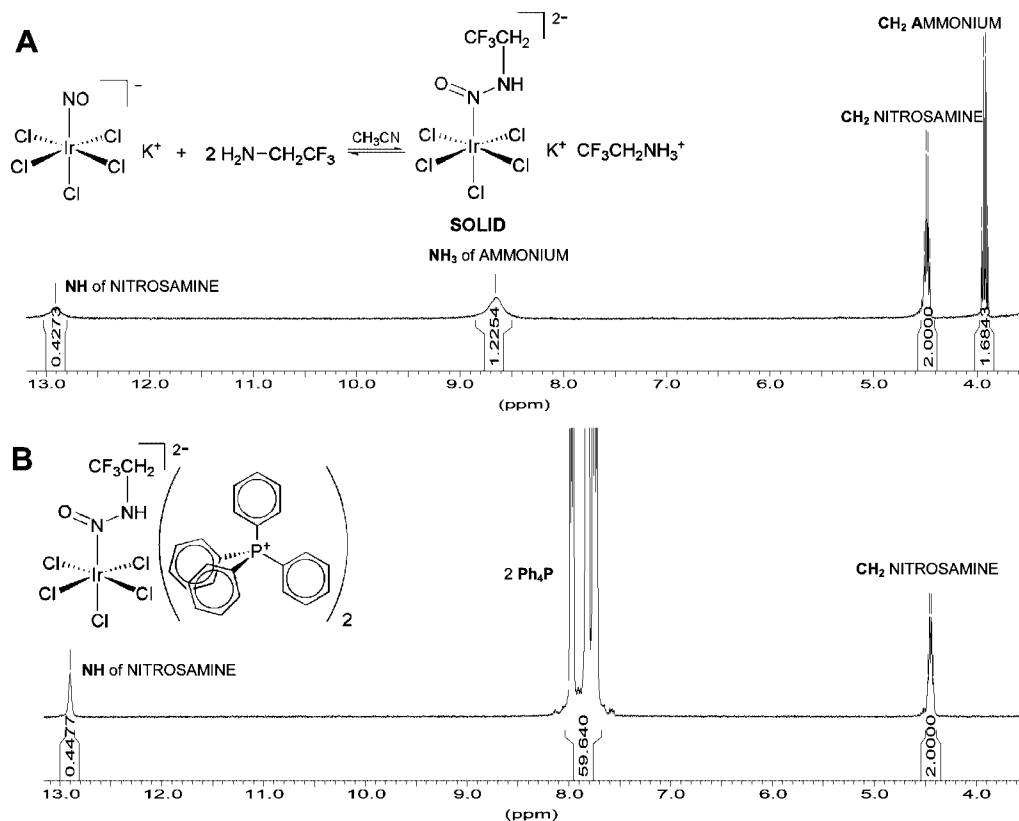


Figure 1. ^1H NMR (DMSO- d_6): (A) 2,2,2-trifluoroethylamine product **1** as K^+ /ammonium salt; (B) 2,2,2-trifluoroethylamine product **1** as PPh_4^+ salt.

Table 1. Temperature Conditions, Products, and Yield for the Reaction of Aliphatic Amines with $\text{K}[\text{IrCl}_5(\text{NO})]$ (solvent: CH_3CN , 2:1 amine:complex ratio)

amine	reaction temperature ($^\circ\text{C}$)	product ^a	yield (%)
2,2,2-trifluoroethylamine	RT	$[\text{IrCl}_5(\text{ONNHCH}_2\text{CF}_3)]^{2-}$ (1)	82
benzylamine	RT	$[\text{IrCl}_5(\text{ONNHCH}_2\text{Ph})]^{2-}$ (2)	90
<i>n</i> -butylamine	-35^b	$[\text{IrCl}_5(\text{ONNHC}_4\text{H}_9)]^{2-}$ (3)	78
cyclopropylamine	-35^c	$[\text{IrCl}_5(\text{ONNH}(c\text{-CHCH}_2\text{CH}_2))]^{2-}$ (4)	92
9-octyladenine	RT	$[\text{IrCl}_5(\text{ONNHC}_{13}\text{H}_{19}\text{N}_4)]^{2-}$ (5)	75

^a In all cases the counterions are $\text{K}(\text{NH}_3\text{R})$, where NH_3R is the ammonium salt of the corresponding amine. ^b Products obtained at RT: $\text{N}_2(\text{g})$, *n*-butyl alcohol, $\text{KNH}_3\text{C}_4\text{H}_9[\text{IrCl}_5(\text{ONNHC}_4\text{H}_9)](\text{s})$ (20–30%), $\text{KNH}_3\text{C}_4\text{H}_9[\text{IrCl}_5(\text{NH}_2\text{C}_4\text{H}_9)](\text{s})$. ^c Products obtained at RT: $\text{N}_2(\text{g})$, cyclopropyl alcohol, ring-opening derivatives, traces of $\text{KNH}_3(c\text{-CHCH}_2\text{CH}_2)[\text{IrCl}_5(\text{ONNH}(c\text{-CHCH}_2\text{CH}_2))]$ and $\text{KNH}_3(c\text{-CHCH}_2\text{CH}_2)[\text{IrCl}_5(\text{CH}_3\text{CN})] \cdot x\text{CH}_3\text{CN}(\text{s})$ (50%).

reporting evidence that the decomposition of a single primary (*Z*)-alkanediazoate was 2600 times greater than its *E* analogue.³² It must be noted that the conformation is *syn* with respect to the nitrosamine itself (Figure 4), but is *anti* to the $[\text{IrCl}_5]^{2-}$ fragment. In that sense, both bulky groups—the $[\text{IrCl}_5]^{2-}$ moiety and the R fragment—are placed as far as possible in order to diminish steric repulsions (see Figure 4), which is the main factor that could explain the higher relative stability of the *syn* conformers.

In order to analyze conformer stabilities, DFT calculations *in vacuo* and applying a solvent model (PCM) were performed on the nitrosamine complexes. A phenyl analogue was included in order to compare the results obtained for the aliphatic amines against an aromatic compound. The stabilization energies found by DFT calculations in acetonitrile for the *syn* conformers with respect to the *anti* ones were between 4 and 14 kcal mol⁻¹ (Figure 5; for the *in vacuo* results see the Supporting Information). The different values obtained for the various complexes

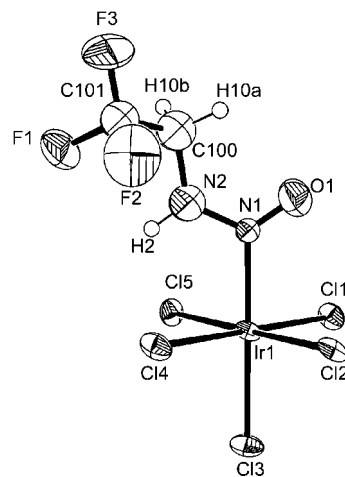


Figure 2. X-ray crystal structure and atom numbering for $[\text{IrCl}_5(\text{N-nitroso-2,2,2-trifluoroethylamine})]^{2-}$ (**1**). Thermal ellipsoids are drawn at the 50% level.¹⁴

(31) Cossi, M.; Barone, V.; Cammi, R.; Tomasi, J. *Chem. Phys. Lett.* **1996**, *255*, 327.

(32) Ho, J.; Fishbein, J. C. *J. Am. Chem. Soc.* **1994**, *116*, 6611.

could be explained by analyzing the steric repulsion generated by the organic groups next to the $\text{HN}-\text{N}=\text{O}$ moiety. Notice

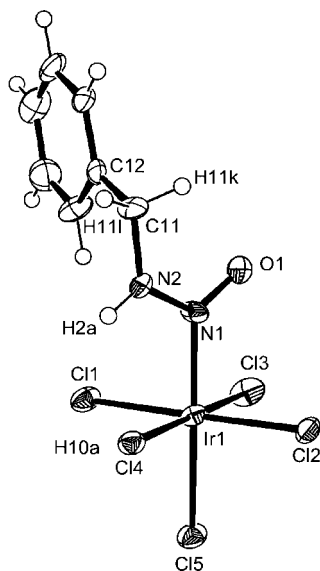


Figure 3. X-ray crystal structure and atom numbering for $[\text{IrCl}_5(\text{N-nitrosobenzylamine})]^{2-}$ (**2**). Thermal ellipsoids are drawn at the 50% level.

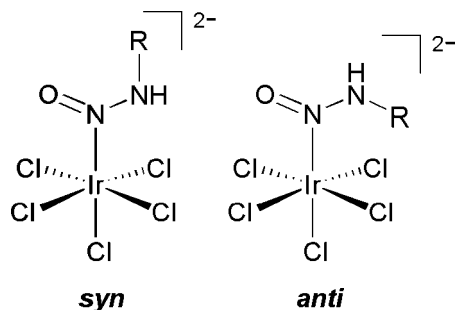


Figure 4. Coordinated nitrosamine conformers.

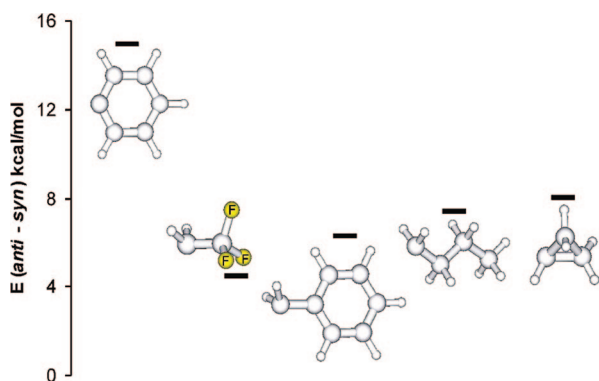
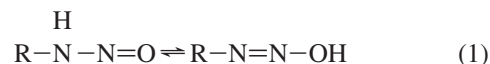


Figure 5. DFT-calculated conformer energy difference ($E(\text{anti-syn})$) in kcal/mol in acetonitrile for the nitrosamine complexes **1** to **4** (B3LYP, DZVP basis sets for N, O, C, H, Cl; LANL2DZ basis set and pseudopotential for Ir, PCM model for acetonitrile). Only the organic residues are shown.

that the higher energy difference value was observed for the phenyl ring substituent followed by the value obtained for the cyclopropyl ring, both being rigid groups, although the second is less voluminous. For the adenine derivative, the *anti* conformer always converged into the *syn* one. This observation is consistent with the fact that its structure could be considered as the most voluminous of all the studied compounds.

To analyze the *N*-nitrosamine \leftrightarrow diazoic acid tautomeric equilibria (eq 1), optimization of the different structures was

performed by DFT calculations *in vacuo* and applying a solvation model. In Figure 6, all the optimized structures corresponding to the nitrosamines and diazoic acids complexes are shown.



As it was already introduced, X-ray data showed that the nitrosamines and not the diazoic acids were the most probable structures for the crystallized precipitated products. However, diazoic acids turned out to be stable local minima in the DFT calculations. In Table 2 relevant DFT-calculated and experimentally determined angles and distances data for **2** are shown. The calculated structural parameters for the corresponding diazoic acid are also included. The calculated DFT values for the remaining coordinated nitrosamines along with the X-ray experimental data for **1**¹⁴ may be found in the Supporting Information.

Comparing the X-ray data and the DFT results for compound **2**, it can be seen that the calculations are in very good agreement with the experimental data. In addition, the data also confirm the correct convergence of the crystallographic X-ray data to an *N*-nitrosamine structure instead of a diazoic acid one. Consequently, it is possible to establish comparisons along the different nitrosamine compounds based just on DFT structural parameters. For instance, parameters related to the N–N and N–O bonds are the most sensitive since double bonds are significantly shorter than single bonds and present different bond angles. Experimental bond values correlate better with the *N*-nitrosamine structures than the diazoic acid ones. Larger differences can be pointed out when relevant angles of diazoic acid structures are compared with the experimental ones. So, coincident with the X-ray data, DFT calculations show that the nitrosamine structure would be the best assignment for the reaction products in the solid state. Energetic value comparison between both derivatives will be shown in the nitrosamine mechanism discussion section.

Experimental FTIR frequencies found for $\nu(\text{N-H})$ were about 3180 cm^{-1} and for $\nu(\text{H-N-N-O})$ between 1547 and 1439 cm^{-1} (see Experimental Section). $\nu(\text{H-N-N-O})$ data have been clearly confirmed through isotopic ^{15}N labeling of the “NO” nitrogen atom. No bibliographic data are available for coordinated primary nitrosamines, but these values correlate considerably well with free secondary nitrosamine frequencies: for $\nu(\text{N-N-O})$ the values are between 1550 and 1425 cm^{-1} and for $\nu(\text{N-N})$ between 1150 and 930 cm^{-1} .³³ In addition, normal-mode analyses were performed to obtain computational data that helped to confirm all the signal assignments and modes (see Supporting Information).

Stability and Reactivity of the Coordinated Nitrosamines. On the basis of the discussion started in the previous section, it is possible to make some preliminary conclusions about the coordinated nitrosamine stability by analyzing the required temperatures to observe the best product yields. While good yields for **1**, **2**, and **5** were obtained at RT, for **3** and **4** good yields were only possible by working at temperatures lower than $-20 \text{ }^\circ\text{C}$. For the last two cases, the RT reaction proceeded up to the formation of the diazonium salts and their subsequent decomposition, facilitated by the higher solubility of these compounds with respect to the nitrosamines (Scheme 2). Quick extraction of the supernatant containing $\text{OH}^-/\text{H}_2\text{O}$ produced by

(33) Lin-Vien, D.; Colthup, N. B.; Fateley, W. G.; Grassetti, J. G. *The Handbook of Infrared and Raman Characteristic Frequencies of Organic Molecules*; AP, Inc.: San Diego, CA, 1991; p 194.

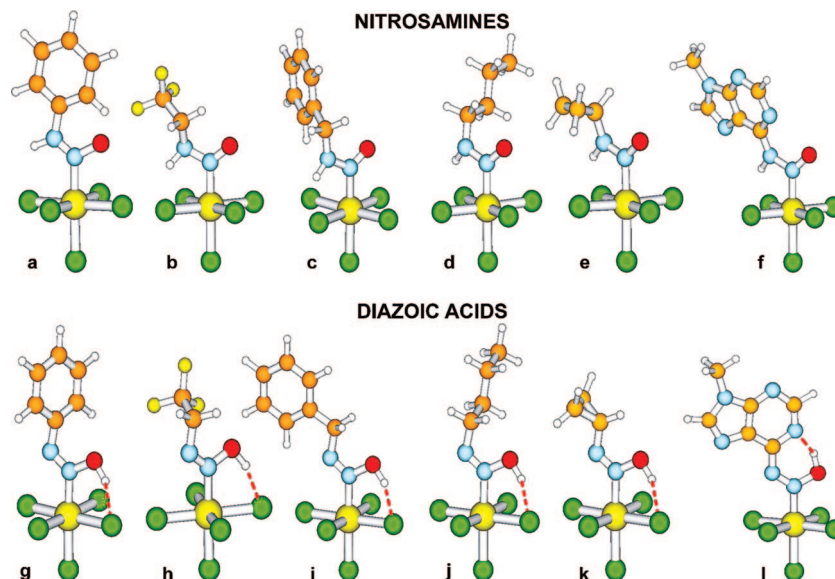


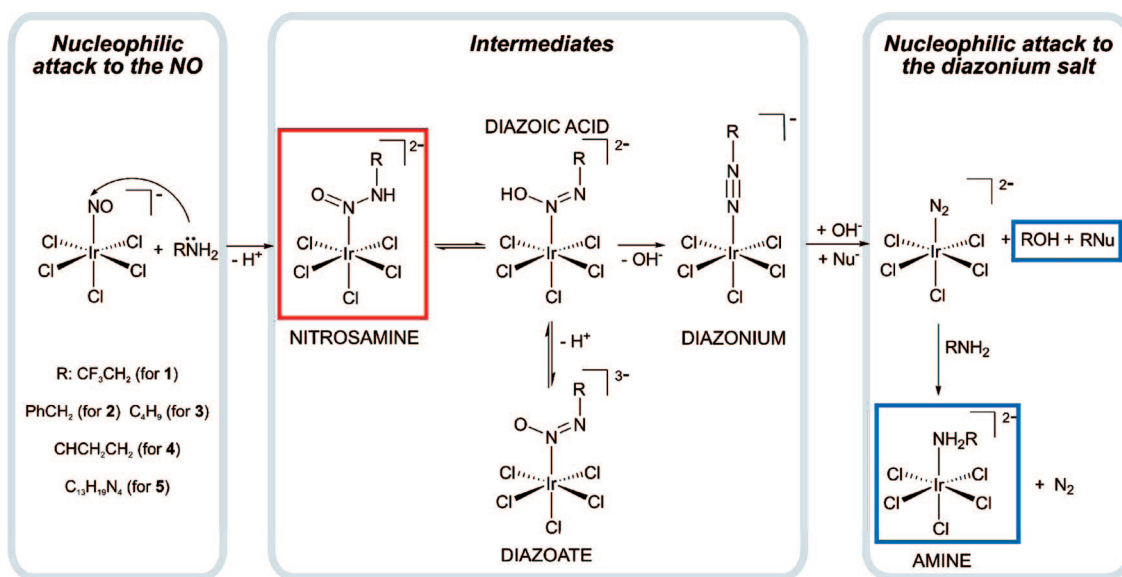
Figure 6. DFT-optimized structures for coordinated nitrosamines (a–f) and diazoic acids (g–l) (B3LYP, DZVP basis sets for N, O, C, H, Cl; LANL2DZ basis set and pseudopotential for Ir); phenyl (a and g), 2,2,2-trifluoroethyl (b and h), benzyl (c and i), *n*-butyl (d and j), cyclopropyl (e and k) and 9-methyladenyl (model for the 9-octyladenyl) (f and l). For the g to l structures an intramolecular H bond interaction is shown with dotted lines.

Table 2. Experimental and DFT (B3LYP, DZVP basis sets for N, O, C, H, Cl; LANL2DZ basis set and pseudopotential for Ir) Optimized Structural Parameters for $\text{syn-}[\text{IrCl}_5(\text{N-nitrosobenzylamine})]^{2-}$ and Calculated Values for $\text{syn-}[\text{IrCl}_5(\text{diazoic benzylic acid})]^{2-}$ (distances are in Å and angles in deg)

	$d(\text{IrN})$	$d(\text{NN})$	$d(\text{NO})$	$d(\text{NH})$	$d(\text{OH})$	$d(\text{NC})$	$d(\text{IrCl}^{\text{trans}})$	$\angle(\text{IrNO})$	$\angle(\text{IrNN})$	$\angle(\text{CNN})$
X-ray parameters ^a	2.000	1.316	1.232	0.880		1.459	2.366	125.84	117.28	122.09
DFT ^b										
$\text{syn-}[\text{IrCl}_5(\text{PhCH}_2\text{RNHNO})]^{2-}$ (nitrosamine)	2.003	1.344	1.228	1.038		1.436	2.427	128.27	115.52	121.84
$\text{syn-}[\text{IrCl}_5(\text{PhCH}_2\text{RNNOH})]^{2-}$ (diazoic acid)	2.022	1.240	1.383	1.017		1.450	2.414	117.61	126.83	118.20

^a Data for $(\text{PPh}_4)_2(\text{syn-}[\text{IrCl}_5(\text{N-nitrosobenzylamine})]) \cdot 3\text{H}_2\text{O}$. ^b *In vacuo* calculations.

Scheme 2. Nitrosation of Primary Amines: Nucleophilic Attack to NO^+ , Nitrosation Reaction Intermediates, and Products Originated from Nucleophilic Attack to the Diazonium Salt (blue box); *N*-Nitrosamines Are Stabilized, Allowing Their Isolation (red box)



the reaction itself partially avoided the nitrosamine decomposition. In the case of **2**, the formation of benzyl alcohol and amine complex was observed when the nitrosamine was kept in the presence of the supernatant during one week, while for **1** or **5** the nitrosamine remained unaltered during weeks or months. The amine complexes that in general precipitate from the media are produced by substitution of the very labile coordinated

nitrogen molecule by the excess of amine present (see right side of Scheme 2). Both products, coordinated amine and alcohol, were observed by ¹H NMR for **1** to **4** and have been isolated for **2** and **3**. Decomposition products derived from **5** are still under analysis. As it was presented before, for the coordinated *N*-nitrosocyclopropylamine (**4**), a variety of decomposition products were found: ones originated by nucleophilic attack to

the diazonium ion or to the alkyl cation and others produced by elimination reactions that occurred in either the unaltered or opened cyclopropyl ring. Apart from these compounds, the precipitate $\text{KNH}_3(c\text{-CHCH}_2\text{CH}_2)[\text{IrCl}_5(\text{CH}_3\text{CN})] \cdot x\text{CH}_3\text{CN}$, resulting from the displacement of the organic ligand by a solvent molecule, was also found. This nitrosamine (**4**) was the only one of the analyzed derivatives that showed this behavior. The information found in the literature shows that traditional nitrosation reactions² of cyclopropylamine result in the formation of several products, like the ones found in this reaction.³⁴

Analyzing the fact that for most of the cases unrearranged alcohols were exclusively observed as nitrosamine decomposition products, two important conclusions could be pointed out. The first one is that, unless in the case of **4**, due to the absence of any organic chloride products, the Ir–Cl bond could be considered as nonlabile, showing the outstanding inertness of the $[\text{IrCl}_5]^{2-}$ unit. A different situation was found when 2,2,2-trifluoroethylamine or *n*-butylamine reacted with $[\text{Ru}(\text{bpy})_2\text{Cl}(\text{NO})]^{2+}$: the chloride derivatives 1-chloro-2,2,2-trifluoroethane and 1-chlorobutane, respectively, were found as the main reaction products.^{12e} The same was observed when hydrochloric acid solutions were added to an aqueous solution of the here-presented coordinated nitrosamines (see later). The second conclusion to be pointed out is related to the stabilization experienced by the diazonium ions when coordinated to $[\text{IrCl}_5]^{2-}$. Unrearranged alcohols found as products can only be attributed to a concerted nucleophilic attack of hydroxide ion to the coordinated diazonium ions; if they were released, they would produce rearranged and elimination products (Scheme 1 and ref 12).

The addition of strong acids accelerates the decomposition of the nitrosamines. The high stability of **1** was demonstrated when practically no changes were observed during weeks after adding acetic acid or a few hours after the addition of concentrated solutions of strong acids such as hydrochloric (HCl), trifluoroacetic (TFA), or perchloric acid (HClO_4). Products formed in the presence of the mentioned acids were analyzed by ^1H NMR and by GC-MS (see Table 3). Together with the nucleophilic attack products, free amines were also observed probably due to hydrolysis of the amine complexes. Another consequence of the presence of acid was related to the formation of rearranged products detected for the more labile nitrosamines, the ones derived from **3** and **4**. In the case of the cyclopropyl derivative **4**, allyl alcohol was the major product, and for the *n*-butyl derivative **3**, small quantities of 1-butene showed that probably a fraction of the nitrosamine or diazonium ion was also labilized, resulting in these products. The mechanism of this reaction will be discussed in the next section.

The products obtained either when the coordinated nitrosamines are attacked by strong acids or when they are kept in the presence of the reaction supernatants are presented in Table 3. The corresponding alcohols are in most cases the major products, and as it was already mentioned, amines were always detected. Other products from nucleophilic attack were observed. Alkyl chlorides, trifluoroacetates, and alkyl iodides were detected in the presence of HCl, TFA, and TFA/I⁻, respectively. The generation of esters could be attributed to the nucleophilic attack of the trifluoroacetate ion. Rearranged products, allyl alcohol and 1-butene, were only observed for the most labile nitrosamines. In the particular case of **4**, this observation was promoted by the stability of the allyl radical.

Table 3. Products Obtained from the Reaction of the Coordinated Nitrosamines $\text{KNH}_3\text{R}[\text{IrCl}_5(\text{NHNOR})]$ in the Presence of Strong Acids or the Supernatant Generated in their Synthesis

condition	products detected by ^1H NMR and/or GC-MS ^a
solid nitrosamine kept in contact with the CH_3CN supernatant	RCH_2OH , $[\text{IrCl}_5(\text{RCH}_2\text{NH}_2)]^{2-}$ in a 1:1 ratio for 1 , 2 , 3 allyl alcohol, cyclopropyl alcohol, $[\text{IrCl}_5(\text{RCH}_2\text{NH}_2)]^{2-}$ in a 0.5:0.5:1 ratio for 4
HCl	RCH_2OH , RCH_2Cl , $\text{RCH}_2\text{NH}_3^+$ for 1 , 2 , 3 in an approximate ratio of 0.9:0.1:1; also found 1–5% of 1-butene for 3 allyl alcohol, cyclopropyl alcohol, cyclopropylamine in a 0.75:0.25:1 ratio for 4 9-octyladenine, cloro-9-octyladenine, and unknown products for 5
DCI	RCD_2OD , RCD_2Cl for 1 , 2 (confirmed by the absence of the expected signal) ^b
CF_3COOH	RCH_2OH , $\text{RCH}_2\text{OC}(\text{O})\text{CF}_3$, $\text{RCH}_2\text{NH}_3^+$ for 1 , 2 , 3 in an approximate ratio of 0.7:0.3:1; also found 1–5% of 1-butene for 3 allyl alcohol, cyclopropyl alcohol, cyclopropylamine in a 0.7:0.3:1 ratio for 4 9-octyladenine and unknown products for 5
$\text{CF}_3\text{COOH/KI}$	RCH_2OH , $\text{RCH}_2\text{OC}(\text{O})\text{CF}_3$, RCH_2I , $\text{RCH}_2\text{NH}_3^+$ for 1 , 2 , 3
HClO_4	RCH_2OH , $\text{RCH}_2\text{NH}_3^+$ for 1 , 2 , 3 in an approximate ratio of 1:1 9-octyladenine and unknown products for 5

^a The high volatility of the products obtained from **1** and **4** made the GC analysis very difficult, so this technique was only applied for **2**, **4**, and **5**. ^b These reactions were only performed for **1** and **2**; a discussion about the isotopic replacement will be included in the next section.

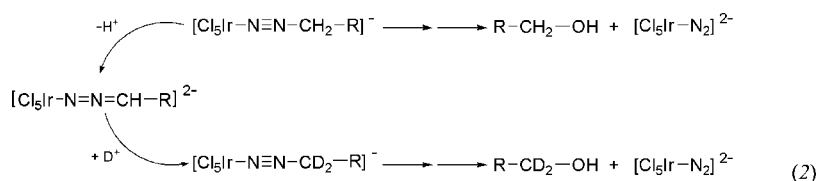
Nitrosation Mechanism. The first step in the nitrosation reaction of primary amines corresponds to the formation of primary nitrosamines (first step, Scheme 2). A very important aspect that must be discussed to understand the complete nitrosation reaction and/or nitrosamine decomposition pathway is the tautomeric equilibrium that could take place in this context (eq 1). When a nitrosating complex such as nitroprusside ($[\text{Fe}(\text{CN})_5(\text{NO})]^{2-}$) or $[\text{Ru}(\text{bpy})_2\text{Cl}(\text{NO})]^{2+12}$ was chosen to perform this kind of reaction, the results were far different from those observed in this work: those reactions did not end in a nitrosamine product. As it was already introduced, for all the nitrosyl complexes studied before in our laboratory, the stability of the diazo compounds produced by nucleophilic addition of amines to coordinated nitrosyl was inferred only through the amounts of unrearranged products detected. For those cases, none of the postulated diazo compounds derived from primary amines could be isolated.¹² In this sense, the nitrosamine could be considered as an intermediate of these reactions, whose separation from the reaction media was feasible due to the inertness of $[\text{IrCl}_5]^{2-}$ and the insolubility of the coordinated nitrosamine.

When the nitrosamine remains in solution, the tautomeric equilibrium involving the diazoic acid can take place (eq 1 and central part in Scheme 2). Then, the diazoic acid is the compound that allows the reaction to evolve to the formation of the diazonium ion. So, taking apart the metal's and coligands' influence, the analysis of the diazoic acid acidity and its proclivity to be dehydrated are the keys to understanding the

(34) (a) Roberts; J. D.; Chambers, V. C. *J. Am. Chem. Soc.* **1951**, *73*, 3176. (b) E. J. Corey, E. J.; Atkinson, R. F. *J. Org. Chem.* **1964**, *29*, 3703.

stability of the nitrosamines. In order to analyze the whole mechanism in terms of the energy of each intermediate compound, several steps must be taken into account: nitrosamine formation (red box in central part of Scheme 2), diazoic acid equilibrium, protonation of the $-OH$ followed by dehydration of the diazoic acid, formation of the coordinated diazonium shown in the central part of Scheme 2, and finally, decomposition of the last compound to form a dinitrogen complex and the corresponding alcohol, mainly through a concerted nucleophilic attack reaction (right side of Scheme 2). Because the last complex is not stable in solution, the amine or a solvent molecule present in the media replaces the nitrogen molecule to give the corresponding compound. As it was presented in the previous section, if no other nucleophiles are added to the reaction mixture, all the nitrosamines exhibit this behavior at the end of the reaction pathway. When acids were added to force the decomposition and to study the derived products, alcohols were the major products again, but other products that originated from nucleophilic attack to the diazonium were also found (Table 3). As it was mentioned, in the central part of Scheme 2 all the steps related to the formation of the coordinated diazonium ions are shown and their decomposition is presented to the right.

Fishbein et al. postulated the existence of another diazo intermediate, which has not been mentioned in the previous paragraph, the diazoalkane ($R-CH=N=N$), based on isotopic labeling kinetic measurements of the decomposition pathway of free (*Z*)-diazoalkanes.³⁵ The incorporation of deuterium into the β -carbon of the final decomposition product of diazo compounds requires the intermediacy of a diazonium ion, which can undergo proton exchange, competing with the hydrolysis (eq 2).



When DCl (c) was used as an acid to force the decomposition of the coordinated nitrosamines, deuterium incorporation was observed (see Table 3). Although proton substitution was complete, the nucleophilic attack pathway cannot be ruled out since the excess acid acts as a driving force for the H^+ exchange and inhibits the nucleophile attack via its protonation.

In order to have more insight into the reaction mechanism, energy calculations of the relevant species *in vacuo* and in acetonitrile using PCM schemes have been performed. In Figure 7, energies for the different intermediates corresponding to all the studied amines are shown together (each value is referred to the corresponding nitrosamine energy, taken as zero). A table showing all the corresponding values for the *in vacuo* and in solvent model calculations is included in the Supporting Information

First of all, it is important to remark that the stabilities for the different nitrosamines agree very well with what has been postulated in the first section based only on experimental evidence: a greater stability of the nitrosamine derived from 2,2,2-trifluoroethylamine (**1**) with respect to the other aliphatic ones (see Supporting Information). Calculations showed that this nitrosamine was around 10^5 kcal/mol more stable than its analogues. With respect to the adenine derivative (**5**), according

to the DFT data, it was even more stable than the trifluoroethylamine one, a fact that is very difficult to prove experimentally since both of them are extremely stable.

The first step in Figure 7 shows that the nitrosamines are more stable than each corresponding diazoic acid. The higher energies that correspond to the diazoate form suggest the possibility that the generation of the diazonium ion could take place directly from the diazoic acid through its protonation ($[\text{RN}=\text{N}-\text{OH}_2]^+$). That fact was indirectly confirmed by DFT calculations because such intermediate structure never converged resulting in the formation of diazonium ion and water. Here, it is important to remark that the coordinated butyldiazonium is the most stable with respect to the corresponding nitrosamine in comparison to the other ones. This observation was also demonstrated experimentally by the fact that although the butyl carbocation is known to be a very unstable species, the products derived from the decomposition of its nitrosamine were almost 100% unrearranged (see Table 3). The diazoalkanes derived from the trifluoroethyl, benzyl, and *n*-butyl amines,³⁶ which are also included in Figure 7, showed energy values around 20 kcal/mol higher than those corresponding to the diazonium ions. These differences demonstrated that both competing pathways are possible, but the diazonium one seems to be the most favorable one at neutral pH. Finally, the very favorable steps depicting the decomposition of each diazonium ion into the free alcohols and nitrogen complexes are found to the right in Figure 7. For cyclopropylamine, cyclopropyl alcohol and the major product found experimentally, allyl alcohol (at lower energy), were both included. The adenine derivatives were included in order to compare all the compounds studied in this work, but as it was already mentioned, the identity of the decomposition product obtained after adding acids to the coordinated nitro-

samine is still unknown. For the DFT calculations the chosen final species was 3-methylhypoxantine, the tautomer of the corresponding 3-methylpurinol.

Some amines form very stable carbocations. Consequently, the dissociation of their diazonium salt complexes into the corresponding species and nitrogen complex is highly favored. Therefore, for such cases, smaller dissociation energies of the $N-C$ bonds are expected. In addition, once the carbocations are released to the media, the observed behavior is the same as that found for the free aliphatic diazonium salts: they are subject to nucleophilic attack and to rearrangement and subsequent nucleophilic attack or elimination reactions (Scheme 1). For those cases, Scheme 2 must be completed with competing reactions shown in Scheme 3.

DFT calculations were also performed to illustrate in a quantitative way the stability of the carbocations and their influences on the coordinated diazonium salt complexes. Table 4 shows the calculated $C-N$ bond dissociation energy values as well as relevant structural parameters for the studied coordinated diazonium salt products. Results of some compounds coordinated to $[\text{Fe}(\text{CN})_5]^{3-}$ are also included in order

(35) Finneman, J. I.; Fishbein, J. C. *J. Am. Chem. Soc.* **1996**, *118*, 7134.

(36) These diazoalkanes were the only ones tested for deuterium incorporation by Fishbein et al. (refs 32 and 35).

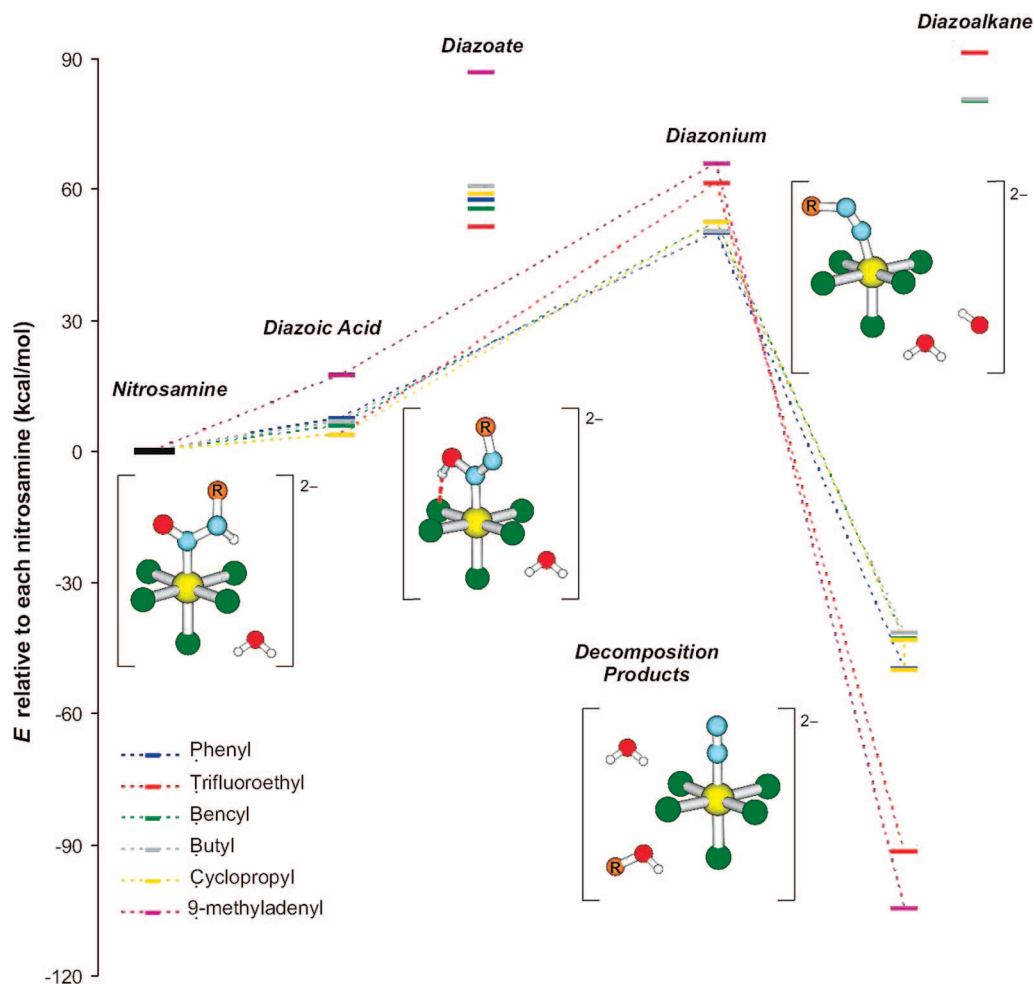
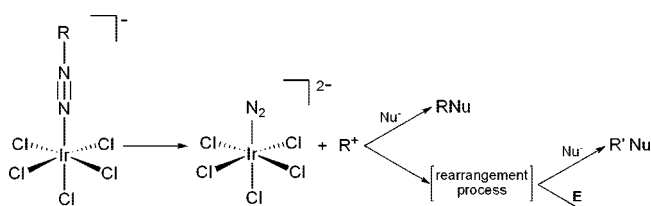


Figure 7. DFT-calculated energies (kcal/mol) in acetonitrile (PCM model) for the proposed intermediates of the nitrosation reaction (the most relevant ones are depicted in square brackets).

Scheme 3. Competing Pathways to the Concerted Nucleophilic Attack to the Coordinated Diazonium Ion^a

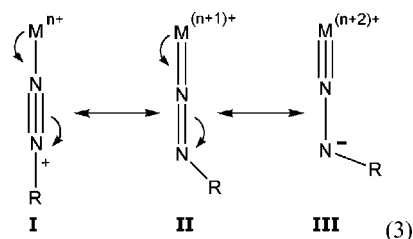


^aNucleophilic attack to the carbocation is indicated above and rearrangement process results are depicted below. R' represents rearranged R, R'' represents the products obtained through elimination reactions (E).

to establish pertinent comparisons. Here again, a phenyl derivative was also taken into account to complete the analysis.

The computed results clearly show the significant differences that exist between diazonium ions coordinated to $[\text{Fe}(\text{CN})_5]^{3-}$ or $[\text{IrCl}_5]^{2-}$. Regarding the C–N bond dissociation energy values, iron compounds were more stable than their iridium analogues. The stabilization of these positive ligands can be understood in terms of the possibility of charge delocalization: three different resultant resonant structures, **I**, **II**, and **III**, are indicated in eq 3. In the cases where back-donation from the metal center into the π^* orbital of the diazonium ion is more significant, the delocalization would be considerably favored.

Taking into account some structural parameters showed in Table 4, it can be seen that back-donation is more efficient for the iron compounds where a larger electronic density is available due to the presence of electron-rich cyanides. The very sensitive $d(\text{NN})$ distances could be used as a parameter for quantifying this fact; in the case of the iron compounds the resulting values were found to be higher than for each corresponding iridium analogue. Calculated charges also demonstrate important differences between both nitrogen atoms present in the diazonium ion ligand ($-\text{N}\equiv\text{N}$). In all cases the nitrogen atom bound to the organic structure presents lower charges, even negative ones for the iron systems, in comparison with the nitrogen atom bound to the metal.



The back-bonding effect could also be understood comparing structural parameters and charges of the diazonium metal complexes with those corresponding to the free ions, where for the latter the C–N–N moieties are practically linear ($\angle(\text{CNN}) \approx 180^\circ$) and show a shorter N–N bond distance (and much more

Table 4. Calculated^a C–N Bond Dissociation Energy and Structural Parameters for [ML₅(diazonium)]ⁿ⁻ Products; M, L, n: Fe, CN, 2 or Ir, Cl, 1

diazonium product	bond dissociation energy (<i>in vacuo</i>) (kcal/mol)	bond dissociation energy (PCM) (kcal/mol)	M	NPA ^b charges		<i>d</i> (MN) (Å)	<i>d</i> (NN) (Å)	<i>d</i> (CN) (Å)	∠(MNN) (deg)	∠(CNN) (deg)
				N(–M or not bound)	N(–C)					
[Fe(CN) ₅ (N ₂ Ph)] ²⁻	286.05	49.34	–0.183	0.219	–0.045	1.662	1.187	1.421	175.4	127.2
[Fe(CN) ₅ (N ₂ CH ₂ CF ₃)] ²⁻ ^c	308.12	49.65	–0.136	0.193	–0.068	1.693	1.186	1.473	160.1	119.7
[Fe(CN) ₅ (N ₂ CH ₂ C ₆ H ₅)] ²⁻	231.10	7.59	–0.145	0.177	–0.140	1.683	1.179	1.506	169.0	121.8
[Fe(CN) ₅ (N ₂ C ₄ H ₉)] ²⁻	253.03	16.62	–0.178	0.204	–0.033	1.675	1.176	1.492	173.4	123.7
[IrCl ₅ (N ₂ Ph)] ⁻	206.12	38.76	0.809	0.121	0.043	1.806	1.168	1.420	173.8	133.0
[IrCl ₅ (N ₂ CH ₂ CF ₃)] ⁻	221.40	33.64	0.817	0.118	0.005	1.820	1.171	1.479	161.2	123.1
[IrCl ₅ (N ₂ CH ₂ Ph)] ⁻	150.12	–14.02	0.801	0.118	0.033	1.820	1.163	1.523	165.8	125.2
[IrCl ₅ (N ₂ C ₄ H ₉)] ⁻	56.45	8.01	0.800	0.138	0.064	1.808	1.160	1.485	178.0	134.5
[IrCl ₅ (N ₂ (<i>c</i> -C ₃ H ₅))] ⁻	161.24	–8.79	0.806	0.122	0.025	1.820	1.168	1.451	164.3	126.6
[IrCl ₅ (N ₂ (C ₆ H ₅ N ₄))] ⁻	171.29	14.09	0.867	0.150	–0.093	1.784	1.176	1.413	171.4	131.0
PhN ₂ ⁺	43.95	40.80		0.129	0.296		1.115	1.383		180.0
CH ₂ CF ₃ N ₂ ⁺	30.79	29.23		0.159	0.383		1.104	1.455		179.8
PhCH ₂ N ₂ ⁺	–15.09	–12.04		0.162	0.310		1.112	1.508		172.9
C ₄ H ₉ N ₂ ⁺	7.11	8.82		0.145	0.336		1.105	1.480		176.5
(<i>c</i> -C ₃ H ₅)N ₂ ⁺	–3.70	–3.83		0.128	0.316		1.110	1.398		179.7
(C ₆ H ₅ N ₄)N ₂ ⁺	11.95	11.85		0.133	0.340		1.110	1.418		180.0

^a B3LYP, DZVP basis sets for N, O, C, H, Cl and LANL2DZ basis set and pseudopotential for Ir. ^b See ref 30. ^c Although this amine does not react with the iron complex, this diazonium salt was included in order to obtain complete comparisons.

positive charges on both nitrogen atoms. It can be concluded that, in general, structures **II** and **III** are predominant with respect to structure **I** for both series of diazonium ions coordinated to the metal, while structure **I** is assigned to the free ones.

In addition, the nature of the organic skeletons generates important variations for the dissociation energies along each series through the stabilization of the free carbocations. Radicals such as benzyl and cyclopropyl (or allyl), clearly contribute to favor the diazonium ion C–N bond breakage. As expected, dissociation energies corresponding to these derivatives were shown to be significantly lower than for the rest of the group.

Calculations also show that for all the coordinated diazonium ions ΔE for their C–N bond dissociation reaction in vacuum are much higher than for the free ions. However, in the presence of a solvent (such as acetonitrile) the situation is reversed in some cases, or both values are practically the same for others (for example, [IrCl₅(N₂C₄H₉)]⁻ vs N₂C₄H₉⁺). This is mainly due to a charge stabilization effect: the dielectric solvent more effectively stabilizes the doubly or triply charged iridium or iron products than the singly or doubly charged corresponding diazonium ion complexes. The opposite situation occurs for the decomposition reactions of the coordinated diazonium ions derived from [Ru(bpy)₂Cl(NO)]²⁺ when a solvent model is taken into account; for these cases the singly charged products are unstabilized with respect to the corresponding doubly charged precursors.^{12b,e} Consequently, the inclusion of the solvent in the iridium and iron systems promotes the coordinated diazonium ion decomposition; this effect was much more important for the ones coordinated to the metals than for the free ions. Nevertheless, back-bonding effects and the characteristic inertness of iridium in particular were shown to be very important factors in conferring stability to the diazonium ion derivatives.

Conclusions

Experimental and computational results previously found in our laboratory have shown the ability of some iron and

ruthenium compounds to stabilize diazonium ions.¹² In those cases, the stabilization of the diazo compounds through coordination could be inferred by analyzing the unrearranged to rearranged product ratio for the nitrosation reactions of aliphatic primary amines by transition metal nitrosyls.

In this work the capability of the [IrCl₅]²⁻ unit to stabilize nitrosamines and diazonium compounds has been shown. The isolation and full characterization of unstable compounds such as primary nitrosamines derived from several aliphatic amines was only possible due to the presence of this particular moiety. The outstanding stabilization effect of this iridium coordination sphere was also observed when the forced or spontaneous decomposition of the coordinated primary nitrosamines took place through clean reactions giving rise only to unrearranged nucleophilic attack products. This fact clearly shows a very strong stabilization of the diazonium ion coordinated to the studied iridium moiety, which is attacked by nucleophiles present in the media through concerted mechanisms.

Therefore, [IrCl₅(NO)]⁻ was shown to be an excellent reagent with several important qualities. Concerning its reactivity, this nitrosyl is considered the most reactive ever known,^{16b} giving the possibility to react with a huge variety of nucleophiles, and finally, it is important to remark again on its capacity to stabilize diazo derivatives.

Acknowledgment. This work was supported by the ANPCYT, CONICET, UBA, and Fundación Antorchas. Thanks are due to Prof. David Milstein for his help with the X-ray facilities.

Supporting Information Available: Tables and graphics containing DFT calculated structural parameters, energy values and normal mode analysis for all the nitrosamines and some experimental data comparisons are included. This material is available free of charge via the Internet at <http://pubs.acs.org>.

OM700985H